Proceedings of the 2011 IEEE
International Conference on Robotics and Biomimetics
December 7-11, 2011, Phuket, Thailand

New Method for Slip and Tire Force Estimation of Wheeled Mobile Robot on Inclined Terrain

Xiaorui Zhu, Chunxin Qiu, Leiming Guo, Yanmin Zhang

***Abstract*—This paper introduces a new method, based on extended Kalman filter (EKF), to estimate wheel slip and tire forces for a four-wheel drive mobile robot on rigid and continuously varying inclined terrain. The longitudinal and lateral forces are both considered in the proposed method. An empirical tire-terrain model from Pacejka's Magic Formula is used to represent the true model of the contact patch force. Simulation results show that the proposed technique can estimate the tire forces and the slip ratio effectively when robot is traveling on simulated inclined surface.**

Index Terms: Mobile robot, Tire force, Slip ratio, EKF

I. Introduction

Wheeled mobile robots are the most dominate platforms for many indoor and outdoor applications because of their fast mobility and simple mechanism. Traditionally, the wheeled robot is considered to posses the ideal dynamic performance. However, when the traction force is not able to compensate for the force applied by the wheel, the linear velocity of the mobile robot becomes slower than the ground velocity. This phenomenon is called wheel slip that limits the traction ability of the robot. In most outdoor environments, wheel slip always occurs and varies when the robot is traveling on the different ground surfaces. In order to evaluate the mobility of the wheeled robot on different inclined terrains, this paper proposes a new method to estimate the tire forces, the slip ratios and their relationships.

Many works have been done so far to estimate the traction loss by estimating the wheel slip. Wong and Reece [1] designed a tire-terrain model to predict the performance of driven and towed rigid wheels operating at constant linear speed in deformable terrain. Ignemma also implemented some fusion techniques to increase overall detection accuracy [2-4]. Ray *et al.* [5-7] estimated the net traction and resistive wheel torques through extended Kalman-Bucy strategy (EKBF) which approved to be suitable either on rigid or deformable terrain. Yoshida *et al.* [8][9] proposed a slip-based traction control method which is similar to the anti-slip regulation in the automobile field. A slip-based model is developed for traction mechanics of a tire on the loose soil. No matter rigid or deformed terrain, most of these works assumed the mobile robot traveling on the even and homogeneous ground surface. Ignemma *et al.* [2] model the vehicle on an inclined surface. However, it assumed that the pitch angle and the roll angle remain constant all the time, and only brought the yaw rate into the dynamic equations. On the other hand, most researchers only considered the slip caused by the loss of the longitudinal traction force. But in most scenarios, mobile robots are suffered from both longitudinal and lateral traction losses. The main contributions of this paper, therefore, include the EKF based estimation algorithm considering the traction force losses in the longitudinal and lateral directions, and the application on continuously varying inclined surfaces.

This paper is organized as follows. Robot dynamics is presented in Section II. Slip and tire force estimation algorithm is presented in Section III. Tire-terrain interaction model for rigid inclined terrain is illustrated in Section IV. Simulation results and discussion are presented in Section V. Conclusions are described in Section VI.

This research is supported by the NSF China Grant No. 60905052.

Xiaorui Zhu is the corresponding author with Harbin Institute of Technology Shenzhen Graduate School, Shenzhen, Guangdong 518055, China (e-mail: xiaoruizhu@hitsz.edu.cn).

II. Robot Dynamics

The configuration of a four-wheel drive mobile robot is shown in Fig. 1 and Fig. 2. The robot has two axes and four rubber pneumatic tires and the road is postulated to be rigid. The body coordinate system and geometric parameters are shown in Fig. 2. The net tire force for each axis is composed of the normal component and the longitudinal component. It is assumed that the lumped mass is located at the center of gravity. Hence the robot dynamics can be described as,

$$\dot{v}_{bx} = v_y\gamma + \frac{1}{m}(F_{x1} + F_{x2} + F_{x3} + F_{x4} - W\sin\theta) \quad (1)$$

$$\dot{v}_{by} = -v_x\gamma + \frac{1}{m}(F_{y1} + F_{y2}) \quad (2)$$

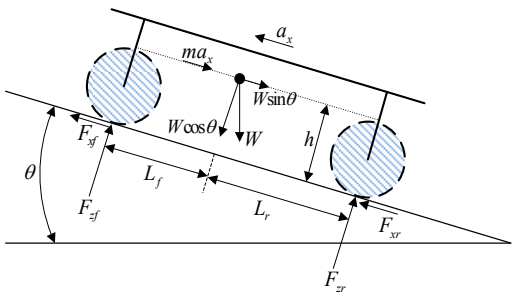

Fig. 1 Side view of the robot

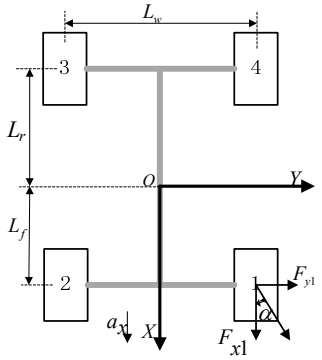

Fig. 2 Top view of the robot.

$$\ddot{\theta} = \frac{1}{I_{yy}}[F_{zr}L_r - F_{zf}L_f - (F_{x1}+F_{x2}+F_{x3}+F_{x4})h] \quad (3)$$

$$\dot{\gamma} = \frac{1}{I_{zz}}[(F_{x2}+F_{x3}-F_{x1}-F_{x4})\frac{L_w}{2} + F_{y1}L_f - F_{y2}L_r - M_{res}\gamma] \quad (4)$$

$$\dot{\omega}_1 = \frac{1}{I_w}(T_1 - T_{rx1} - b_w\omega_1) \quad (5)$$

$$\dot{\omega}_2 = \frac{1}{I_w}(T_2 - T_{rx2} - b_w\omega_2) \quad (6)$$

$$\dot{\omega}_3 = \frac{1}{I_w}(T_3 - T_{rx3} - b_w\omega_3) \quad (7)$$

$$\dot{\omega}_4 = \frac{1}{I_w}(T_4 - T_{rx4} - b_w\omega_4) \quad (8)$$

The m is the total mass, and W is the gravity. The v_{bx} and v_{by} are the body velocities at the longitudinal and lateral directions, respectively. The F_{xi} is the net longitudinal force at i^{th} wheel patch. The F_{y1} and F_{y2} represent the net lateral force components at the front and rear axis, respectively. The F_{zf} and F_{zr} represent the normal forces on the front and rear wheels. The θ represents the pitch angle and γ represents the yaw rate. The ω_i, represent the angular velocity of the i^{th} wheel. The T_i represents the applied torque of the i^{th} wheel. The I_{yy}, I_{zz} are the moment of inertial about the Y axis, and Z axis respectively.

III. Slip and Tire Force Estimation

A. Tire force estimation

In order to estimate the tire forces, a estimator is presented here based on the extended Kalman Filter (EKF) [10]. The estimator state is defined as,

$$\begin{aligned}[x_1, x_2, x_3, x_4, x_5]^T &= [\hat{v}_{bx}, \hat{v}_{by}, \hat{\gamma}, \hat{\theta}, \dot{\hat{\theta}}] \\ [x_6, x_7, x_8, x_9]^T &= [\hat{\omega}_1, \hat{\omega}_2, \hat{\omega}_3, \hat{\omega}_4]^T\end{aligned} \quad (9)$$

where the symbol ^ represents the estimate of a variable. The control input is defined as $u_i = T_i$, i=1-4. The augmented states for the estimator are defined as the estimates of the tire forces and their derivatives:

$$\begin{aligned}[x_{10}, x_{11}, x_{12}, x_{13}]^T &= [\hat{F}_{x1}, \dot{\hat{F}}_{x1}, \hat{F}_{x2}, \dot{\hat{F}}_{x2}]^T \\ [x_{14}, x_{15}, x_{16}, x_{17}]^T &= [\hat{F}_{x3}, \dot{\hat{F}}_{x3}, \hat{F}_{x4}, \dot{\hat{F}}_{x4}]^T\end{aligned} \quad (10)$$

$$[x_{18}, x_{19}, x_{20}, x_{21}]^T = [\hat{F}_{y1}, \dot{\hat{F}}_{y1}, \hat{F}_{y2}, \dot{\hat{F}}_{y2}]^T \quad (11)$$

For normal force calculation, it is assumed that the pitch acceleration of the robot is negligibly small. If the robot is accelerating along the road, it is convenient to represent the effect by an equivalent inertial force known as a "d'Alembert force" denoted by mv_{bx} acting at the center of gravity opposite to the direction of acceleration [11][12]. According to the static equilibrium,

$$F_{zf}(L_f + L_r) - mg\cos\theta L_r + mg\sin\theta h + m\dot{v}_{bx}h = 0 \quad (12)$$

$$-F_{zr}(L_f + L_r) + mg\cos\theta L_f + mg\sin\theta h + m\dot{v}_{bx}h = 0 \quad (13)$$

From the above equations The F_{zf} and F_{zr} can be solved as,

$$F_{zf} = \frac{mg\cos\theta L_r - mg\sin\theta h - m\dot{v}_{bx}h}{L_f + L_r} \quad (14)$$

$$F_{zr} = \frac{mg\cos\theta L_f + mg\sin\theta h + m\dot{v}_{bx}h}{L_f + L_r}. \quad (15)$$

Combing Eq. (1)-(8) and Eq. (14)-(15), the estimate dynamics can be written as,

$$\dot{\hat{v}}_{bx} = \hat{v}_{by}\hat{\gamma} + \frac{1}{m}(\hat{F}_{x1} + \hat{F}_{x2} + \hat{F}_{x3} + \hat{F}_{x4} - mg\sin\hat{\theta}) \quad (16)$$

$$\dot{\hat{v}}_{by} = -\hat{v}_{bx}\hat{\gamma} + \frac{1}{m}(\hat{F}_{y1} + \hat{F}_{y2}) \quad (17)$$

$$\dot{\hat{\gamma}} = \frac{1}{I_{ZZ}}[(\hat{F}_{x2} + \hat{F}_{x3} - \hat{F}_{x1} - \hat{F}_{x4})\frac{L_w}{2} + \hat{F}_{y1}L_f - \hat{F}_{y2}L_r - M_{res}\hat{\gamma}] \quad (18)$$

$$\dot{\hat{\theta}} = \dot{\hat{\theta}} \quad (19)$$

$$\ddot{\hat{\theta}} = \frac{1}{I_{yy}}mh\hat{v}_{by}\hat{\gamma} \quad (20)$$

$$\dot{\hat{\omega}}_1 = \frac{1}{I_w}(T_1 - R_w\hat{F}_{x1} - b_w\hat{\omega}_1) \quad (21)$$

$$\dot{\hat{\omega}}_2 = \frac{1}{I_w}(T_2 - R_w\hat{F}_{x2} - b_w\hat{\omega}_2) \quad (22)$$

$$\dot{\hat{\omega}}_3 = \frac{1}{I_w}(T_3 - R_w\hat{F}_{x3} - b_w\hat{\omega}_3) \quad (23)$$

$$\dot{\hat{\omega}}_4 = \frac{1}{I_w}(T_4 - R_w\hat{F}_{x4} - b_w\hat{\omega}_4) \quad (24)$$

Each tire force from x_{10} to x_{21} is represented as a random walk in the form of Eq. (25) [8].

$$\dot{\hat{F}} = \begin{bmatrix}\dot{\hat{F}}_0 \\ \ddot{\hat{F}}_1\end{bmatrix} = \begin{bmatrix}0 & 1 \\ 0 & 0\end{bmatrix}\begin{bmatrix}\hat{F}_0 \\ \dot{\hat{F}}_1\end{bmatrix} + w \quad (25)$$

$\hat{F}_0$ is the force to be estimated, $\hat{F}_1$ is its first time derivative.

The measurement vector is:

$$z_k = [\gamma, \theta, \dot{\theta}, \omega_1, \omega_2, \omega_3, \omega_4, a_x, a_y, V]^T \quad (26)$$

where a_x , a_y , γ , $\dot{\theta}$ are the measurements of X-axis acceleration, Y-axis acceleration, yaw rate, and pitch rate from IMU. The ω_i is the angular velocity measurement from the wheel encoder. The V is the body velocity of robot. The v_{bx} and v_{by} are measured from IMU. Then the measurement model can be described as,

$$\hat{z} = h(\hat{x}_A, 0) = \begin{bmatrix} \hat{\gamma} \\ \hat{\theta} \\ \hat{\dot{\theta}} \\ \hat{\omega}_1 \\ \hat{\omega}_2 \\ \hat{\omega}_3 \\ \hat{\omega}_4 \\ \hat{v}_{by}\hat{\gamma} + \dfrac{\hat{F}_{x1} + \hat{F}_{x2} + \hat{F}_{x3} + \hat{F}_{x4} - mg\sin\hat{\theta}}{m} \\ -\hat{v}_{bx}\hat{\gamma} + \dfrac{\hat{F}_{y1} + \hat{F}_{y2}}{m} \\ \sqrt{\hat{v}_{bx}^2 + \hat{v}_{by}^2} \end{bmatrix} \quad (27)$$

The tire forces can be therefore estimated by solving Eq. (16) -(24), Eq. (25)and(27).

B. Slip estimation

The linear velocity of the body is ideally equal to the angular velocity of the wheel multiplying the wheel radius. However, when the torques are applied on the wheels to accelerate/break the robot, the linear velocity of the robot and the angular velocity of the wheel may not satisfy this condition. Hence the slip ratio λ is introduced to describe this difference [13][14]. Slip angle α is introduced to describe the angle between the actual movement direction of a rolling wheel and the pointing direction of the combined velocity of the longitudinal velocity and lateral velocity [15-18]. Hence the slip ratio and slip angle can be estimated using Eq. (28)-(29).

$$\hat{\lambda}_i = \begin{cases} \dfrac{\hat{\omega}_i R_w - \hat{v}_{bx}}{\hat{v}_{bx}} \times 100 \quad \text{(for traction)} \\ \dfrac{\hat{v}_{bx} - \hat{\omega}_i R_w}{\hat{v}_{bx}} \times 100 \quad \text{(for braking)} \end{cases} \quad (28)$$

$$\hat{\alpha} = -\arctan(\frac{\hat{v}_{by}}{\hat{v}_{bx}}) \quad (29)$$

IV. TIRE –TERRAIN MODEL FOR RIGID INCLINED TERRAIN

The well-known empirical model, Pacejka's magic Formula, is commonly used to describe the tire-terrain interaction for rigid terrains. This model is applied in this paper to simulate the true values of the slip and tire forces.

Table 1 Parameters in Pacejka's Magic Formula

Symbol	Value	Units	Symbol	Value	Units
b_0	1.8	_	a_0	2.8	_
b_1	0.0034	_	a_1	0.0016	_
b_2	0.004	_	a_2	0.0004	_
b_3	0.3	_	a_3	10	_
b_4	1.5	_	a_4	2.7	_
b_5	0.15	_	a_5	0.15	_
b_6	0.004	_	a_6	0.262	_
b_7	-0.37	_	a_7	-0.37	_
b_8	3.2	_	a_8	3.2	_

The official Pacejka-96 longitudinal force formula is represented as [19],

$$F_x = D_x \sin\{C_x * \tan^{-1}[B_x x + E_x(\tan^{-1}(B_x x) - B_x x)]\} + S_v \quad (30)$$

$$x = 100\lambda + S_h \quad (31)$$

where F_x is the longitudinal tire force, F_z is the total normal force of the robot, λ is the slip ratio, S_h and S_v are the shifting values. The B_x , C_x , D_x and E_x are given by the constants b_0 - b_{10} as,

$$C_x = b_0 \quad (32)$$

$$D_x = b_1 F_z^2 + b_2 F_z \quad (33)$$

$$B_x = \frac{(b_3 F_z^2 + b_4 F_z) e^{-b_5 F_z}}{C_x D_x} \quad (34)$$

$$E_x = b_6 F_z^2 + b_7 F_z + b_8 \quad (35)$$

$$S_h = b_9 * F_z + b_{10} \quad (36)$$

Likewise, the lateral tire force is represented as [19],

$$F_y = D_y \sin\{C_y * \tan^{-1}[B_y x + E_y(\tan^{-1}(B_y x) - B_y x)]\} + S_v \quad (37)$$

$$x = \alpha + S_h \quad (38)$$

where F_y is the lateral tire force, F_z is the total normal force

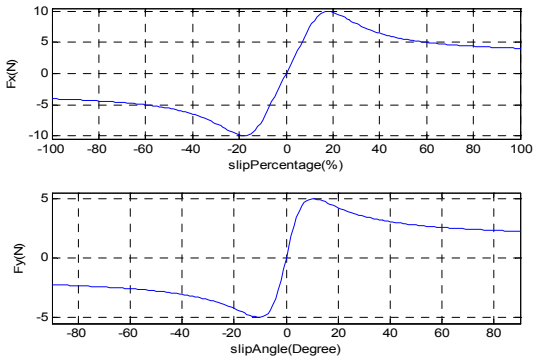

Fig. 3 Force-slip curves

Table 2 List of robot parameters.

Symbol	Description	Value	Units	How to obtain
m	Robot mass	9.67	kg	Direct measurement
I_{zz}	z-axis moment of inertia	0.237	kg-m^2	From 3D Solidworks model
m_w	Wheel mass	0.284	kg	Direct measurement
R_w	Wheel radius	0.0716	m	Direct measurement
L_w	Track width	0.44	m	From 3D Solidworks model
L_f	Front axle distance	0.176	m	From 3D Solidworks model
L_r	Rear axle distance	0.223	m	From 3D Solidworks model
M_{res}	Yaw damping coefficient	0.3	Unit less	Estimation
b_w	Wheel damping coefficient	0.0197	N m/s	Experiment
I_w	Wheel moment of inertia	0.0135	Kg m^2	Experiment

of the robot, α is the slip angle. If β is the inclination angle, the B_y, C_y, D_y and E_y are similarly given by the constants a_0 - a_{13} as,

$$C_y = a_0 \tag{39}$$

$$D_y = a_1 F_Z^2 + a_2 F_Z \tag{40}$$

$$B_y = \frac{a_3 \sin\left(2\arctan\frac{F_Z}{a_4}\right)\times\left(1-a_5|\beta|\right)}{C_y + D_y} \tag{41}$$

$$E_y = a_6 F_Z + a_7 \tag{42}$$

$$S_h = a_9 F_Z + a_{10} + a_8 \beta \tag{43}$$

$$S_v = a_{11} F_Z \gamma + a_{12} F_Z + a_{13} \tag{44}$$

For a flat surface, the values of B, C, D and E remain constant. If the robot is driving on an inclined surface, the parameters B, C, D and E will change over the time because of the varying normal force. However, the parameters a_0 - a_{13} and b_0 - b_{10} keep constant, Table 1. Notice that other parameters not given in Table 1 are all equal to zero. Hence the above equations based on the magic formula can be used to simulate the tire-terrain interaction on inclined terrains. The resulting ideal force-slip curve is shown in Fig. 3.

However, the transient force lagging phenomena always affects the tire forces [17-18, 20-23]. In order to take this effect into account, a non-linear first order equation is introduced as [23],

$$\tau_{lag}\dot{F} + F = F_{stat} \tag{45}$$

where F_{stat} is the static tire force from the quasi-static models, and F is the lagged tire force. The τ_{lag} is the time constant and can be approximated by

$$\tau_{lag} = \frac{L}{V_w} \tag{46}$$

where L is the constant relaxation length, V_w is the time dependent rolling speed. Define that Δt is sample time, F_{ij} refers to the resulting tire force at a particular wheel, and F_{ij_MF96} refers to the tire force calculated from the official Pacejka-96 force. The discrete tire force representation can then be obtained as,

$$F_{ij}(k+1) = (1-\frac{\Delta t}{\tau_{lag}})F_{ij}(k) + \frac{\Delta t}{\tau_{lag}}F_{ij\_MF96} \tag{47}$$

V. Simulation

A. Simulation procedures

The parameters, such as the motor damping coefficients, the wheel inertial, and the noise covariance are obtained before the simulation. The wheel inertia I_w and the damping coefficient b_w are measured experimentally from the response of the wheel angular velocity to a step motor torque command when the wheel is raised off the ground. All the values of the robot parameters are listed in Table 2.

The algorithm in Section III is used to estimate the slip and tire forces while the Magic Formula in Section IV is applied to simulate their true values. The input commands are shown in Fig. 4 with 0.8 N-m for the first 2 seconds, 0.6 N-m for the next 2 seconds, then followed by a right-turn torque for the last 2 seconds with 0.45 N-m on the left two wheels and 0.35 N-m on the right two wheels. That implies a change of the yaw direction in the last 2 seconds. In Fig. 4, left wheel torque inputs are plotted in the solid lines while right wheel torques

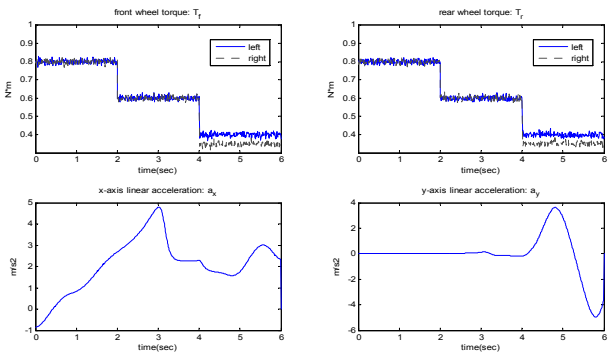

Fig. 4 Input torques and linear acceleration

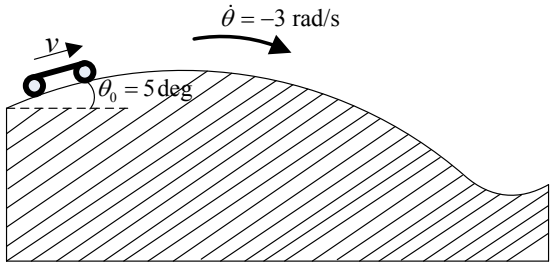

Fig. 5 The varying pitch angle during the robot movement

inputs are plotted in dotted lines. In order to verify the technique discussed in this paper, a continuously varying inclined terrain is simulated by letting the pitch angle of the robot change the values during the robot movement, Fig. 5. The initial pitch angle is 5 degree and its changing rate is -3 deg/sec.

B. Simulation results

According to the algorithms in Section III and IV, the simulation results are shown in Fig. 6-10 where the solid blue lines, the dashed blue ones and the red lines represent the references, the estimated values, the estimation errors respectively.

On this continuously varying inclined terrain, the normal force is varying due to changing of the pitch angle. Fig. 6 shows that the normal forces acting on front wheels and rear wheels are changing while the robot is traveling on the simulated surface. The normal force of the front wheels is increasing while the normal force of the rear wheels is slowing down. Fig. 7 and Fig. 8 indicate that the estimates of the longitudinal force and lateral force can mostly track the reference forces well. It is worth to notice that, in the last few seconds, the tracking error of the lateral force becomes relatively large even though it is still acceptable. It is believed that the sharp turn of the robot has increased the tracking error.

It is indicated by Fig.9 and Fig. 10 that the estimates of the slip ratio and the slip angle can track the reference values as well. Hence the relationship between the longitudinal tire force and the slip ratio is depicted in Fig. 11, which is consistent with the ideal curve. The relationship between the lateral tire force and the slip angle is depicted as well in Fig. 11. However, the curve is not as good as the one in the longitudinal direction possibly because of the transient response resulted from the sharp turn.

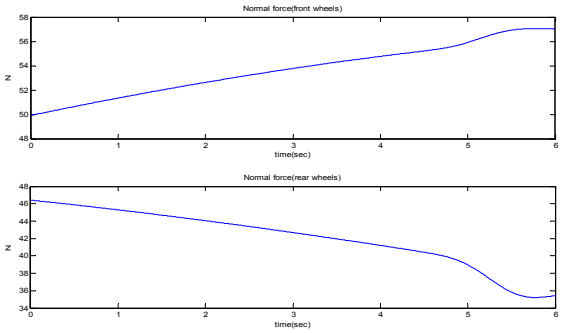

Fig. 6 Normal forces

VI. CONCLUSIONS

This paper presents a new method based on the Extended Kalman Filter (EKF) to estimate the slip and the tire forces for a four-wheel drive mobile robot traveling on the continuously varying inclined terrains. The applied platform is equipped with the wheel encoders, IMU and the inclinometer. A tire-terrain model based on the Pacejka's Magic Formula is used in this paper to provide the reference values of the tire forces. Simulation results validate the proposed technique. Future work will focus on application to the inclined terrain resulting in the varying roll rate of the mobile robot.

REFERENCES

[1] J. Wong, and A. Reece, " Prediction of Rigid Wheels Performance Based on Analysis of Soil-Wheel Stresses, " Part I, Journal of Terramechanics, Vol. 4, pp. 81-98, 1967.

[2] C.C. Ward, K. Iagnemma, " Model-Based Wheel Slip Detection for Outdoor Mobile Robots, " presented at 2007 IEEE International Conference on Robotics and Automation, 10-14 April 2007, Roma, Italy, 2007.

[3] C.C.Ward; K. Iagnemma, " A Dynamic-Model-Based Wheel Slip Detector for Mobile Robots on Outdoor Terrain," *IEEE Transactions on Robotics*, vol. 24, pp. :821 - 831, 2008.

[4] C.C. Ward, K. Iagnemma, " Classification-Based Wheel Slip Detection and Detector Fusion for Outdoor Mobile Robots," presented at 2007 IEEE International Conference on Robotics and Automation, 10-14 April 2007, Roma, Italy, 2007.

[5] L.Ray, D.Brande, and J. Lever, "Estimation of net traction for differential-steered wheeled robots," *Journal of Terramechanics*, vol. 46, pp. 75-87, 2009.

[6] L.Ray, " Nonlinear Estimation of Vehicle State and Tire Forces.

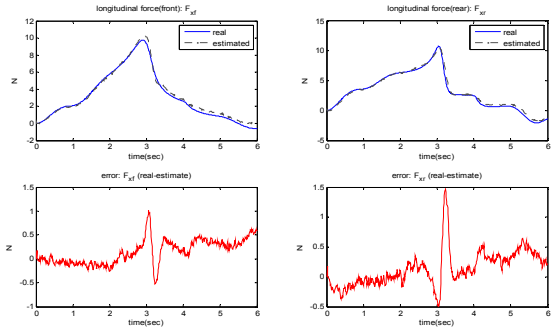

Fig. 7 Longitudinal forces

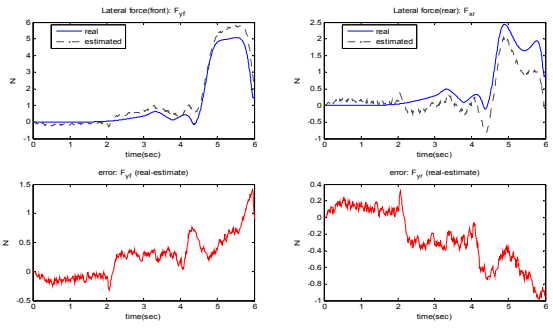

Fig. 8 Lateral forces

American Control Conference," presented at 1992 American Control Conference, 24-26 June 1992, Chicago, IL, USA, 1992.
[7] L.Ray, " Nonlinear Tire Force Estimation and Road Friction Identification: Simulation and Experiments. "Automatica, 33(10), 1819-1833, 1997.
[8] K.Yoshida, H. Hamano, T.Watanabe, " Slip-based Traction Control of a Planetary Rover. " Springer Berlin,2003.
[9] G. Ishigami, A. Miwa, K. Nagatani, K. Yoshida, " Terramechanics-based Model for Steering Maneuver of Planetary Exploration Rovers on Loose Soil," Journal of Field Robotics, vol. 24, pp. 233-250, 2007.
[10] R. F. Stengel, Stochastic optimal control: theory and application. 2nd New York: Wiley; 1993
[11] M. G. Bekker, Theory of land locomotion. Ann Arbor (MI): University of Michigan Press; 1956.
[12] J. Wong,, Theory of Ground Vehicles. New York: Wiley, 2001.
[13] K. Iagnemma, H. Shibly, S. Dubowsky, " On-line terrain parameter estimation for planetary rovers, " presented at 2002 IEEE International Conference on Robotics and Automation, 11-15 May 2002, Washington, DC, USA, 2002.
[14] Pacejka's Magic Formula http://www.racer.nl/reference/pacejka.htm.
[15] H. Pacejka, Tire and Vehicle Dynamics, 2ed. Warrendale, PA: Society of Automotive Engineers, 2005
[16] H. Pacejka, E. Bakker The magic formula Tyre model. In: Proc of the 1st international colloquium on Tyre models for vehicle dynamics analysis; 1991. p. 1–18.
[17] G. Baffet, A. Charara, J. Stephant, " Sideslip angle, lateral tire force and road friction estimation in simulations and experiments, " presented at 2006 IEEE International Conference on Control Applications, 4-6 Oct ,2006, 2002, Munich, Germany, 2006.
[18] Slip angle. (2009, October 25), In Wikipedia, The Free Encyclopedia. Retrieved 06:23, November 10, 2009.
[19] R. Rajamani, Vehicle Dynamics and Control, Springle US, 2006,ch.13.
[20] T. Gillespie, Fundamentals of Vehicle Dynamics. Society of Automotive Engineers, Warrendale, PA. 1992, ch. 1.
[21] G. Baffet, A. Charara, J, " Stephant.Identification of lateral tyre force dynamics using an extended Kalman filter from experimental road test data, " Control Engineering Practice, Vol. 17, pp.357-367, 2009.
[22] D. C. Brande, Estimation of Tire Forces for a Differential Steered Robot. Thayer School of Engineering Dartmouth College, 2007.
[23] W. Liang, Medanic, Jure and Ruhl, Roland, "Analytical dynamic tire model, "Vehicle System Dynamics, vol.46, pp.197-227, 2008.

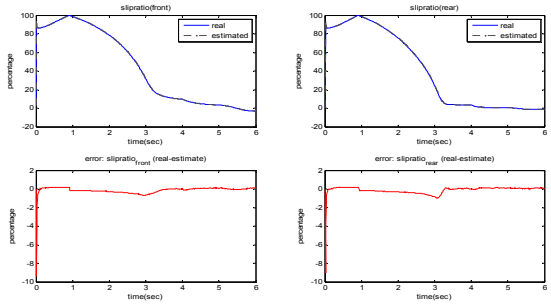

Fig. 9 Slip ratio

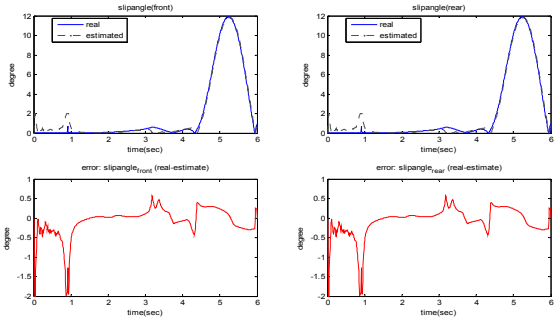

Fig. 10 Slip angle

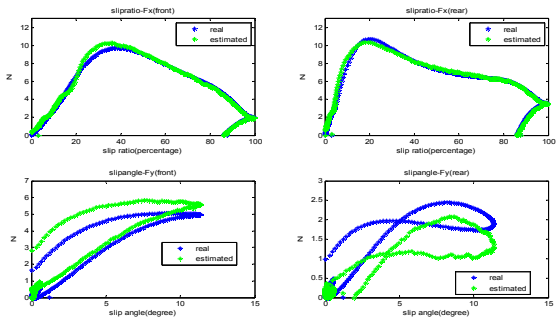

Fig. 11 Force-slip curve